E190Q Lab 2 – Error Characterization of Motion Estimation with Jaguar's Odometry

Benjamin Chasnov
Harvey Mudd College
Claremont, CA
bchasnov@hmc.edu

Samuel Yim
Harvey Mudd College
Claremont, CA
syim@hmc.edu

***Abstract*— In this lab, motion estimation was implemented on the Jaguar robot by using a kinematic model which translates odometry measurements in the local frame to transformations in the global frame. The error of this model was characterized through a series of experiments performed in the lab and on concrete and grass. On all terrains, the Jaguar's estimated position and orientation was compared with its actual measured position. Indoors, odometry-determined rotation was found to have a systematic error of 0.13 radians per radian predicted. In addition, 95% of random error during a rotation of 20π was determined to be within ±5.88 radians. The Jaguar was found to move forward similarly on grass, concrete, and in the lab, with a systematic error of about +0.10m for every 1 meter the Jaguar calculated it traveled forward. This systematic error was used to determine an effective radius of the Jaguar, which can be implemented in future kinematic models to reduce systematic error.**

Keywords—odometry; motion estimation; kinematic modeling; Jaguar robot; error characterization; drift.

I. INTRODUCTION

Mobile robots frequently use odometry to estimate their motion in the global coordinate frame. Since there is no easy method to measure a mobile robot's position instantaneously, one must integrate the local motion of the robot over time. However, the accumulated inaccuracies of motion estimation—systematic and random error—makes determining the robot's position a very difficult task. As a consequence, the errors involved in motion estimation play an important role in mobile robotics. The goal of this lab is to characterize the error involved with using odometry for motion estimation. This error characterization will be useful in localizing and navigating the robot in later labs.

A direct illustration of the issue of error in odometry can be seen in Fig. 1. An LED flashing at 2 Hz was attached to the Jaguar, while a 6 second exposure photo captured its trajectory.

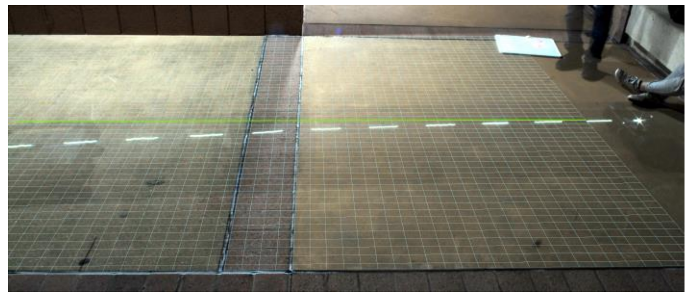

Fig. 1. Trajectory of the Jaguar over 6 seconds, showing the accumulative error. Each white dash represents a time duration of 0.25s, and each grid line represents approximately 5cm.

The dashed white line is the robot's trajectory, and the perspective grid and the green line were added in with Photoshop to show the robot's motion estimation path. Notice the increasing error in the robot's estimation. This is one of the errors we wish to characterize.

A more dramatic representation of odometry error is shown in Fig. 2 below. This figure shows a 20 second exposure photo capturing the Jaguar's trajectory as it accumulatively deviates from its estimated path (shown in white).

Fig. 2. Trajectory of the Jaguar over 20 seconds exposure photo. Each dash represents 0.25 seconds. The white line down the center is the robot's estimated path.

Although the experiments Fig. 1 and Fig. 2 were not conducted rigorously, they demonstrate an absolute necessity for error characterization in mobile robotics odometry. This paper will establish experiments to help characterize this error and understand when and how to be certain about the Jaguar's motion estimation.

II. Background

The Jaguar is a mobile all-terrain navigation robotic platform developed by Dr Robot Inc. It integrates an outdoor GPS, a 9 DOF IMU, a 270° laser range scanner and a low light camera. These sensors can be used to implement autonomous control of the robot. It uses continuous rubber tracks to move. The Jaguar weighs less than 14kg, is compact, rugged and weather resistant.

To use the Jaguar with autonomous control, it needs to know where it is. This can be accomplished by using wheel odometry. Odometry on the Jaguar is estimated by counting wheel revolutions with an optical encoder. By using the wheel revolutions to calculate the change in the robot's local frame, we can determine the change of the robot in its global frame.

An optical encoder works by using a pair of photoemitter and photodetector to measure the revolution of the wheel. The number of encoder counts corresponds to the angular displacement of the encoder wheel. By processing the number of encoder counts, we can determine the rotation of the wheel over a specific time interval, and from that, determine the distance each wheel travelled. Further, once the distance each wheel travels is known, a kinematic model can be used to describe its global translation and rotation.

III. Kinematic Model

To model the kinematics of the Jaguar, a simple wheeled robot is considered. While the rubber tracks of the Jaguar are considerably different from idealized wheels, it was assumed that some effective radius of the Jaguar could be determined that would make the following kinematic model useful for odometry.

Equations (3.1) and (3.2) show how the displacement of each wheel was determined, where Δs_r and Δs_l are shown in Fig. 3, L_{wheel} is the radius of a wheel, Δd_r is the difference between the current and last encoder measurement, and D_{rev} is the number of encoder pulses per wheel revolution.

$$\Delta s_r = 2\pi L_{wheel} \frac{\Delta d_r}{D_{rev}} \tag{3.1}$$

$$\Delta s_l = 2\pi L_{wheel} \frac{\Delta d_l}{D_{rev}} \tag{3.2}$$

Equations (3.3) and (3.4) describe how the overall change in displacement and angle can be determined from the changes in wheel displacement and the radius of the robot. Δs_r, Δs_l, and $2L_{robot}$ are shown in Fig. 3. The Jaguar's effective radius L_{robot} was experimentally estimated to be 0.28m ±0.01m by using a ruler.

$$\Delta\theta = \frac{\Delta s_r - \Delta s_l}{2L_{robot}} \tag{3.3}$$

$$\Delta s = \frac{\Delta s_r + \Delta s_l}{2} \tag{3.4}$$

Equations (3.5) and (3.6) describe how the global Δx and Δy components can be found from the total distance Δd traveled. Fig. 4 illustrates these components. The assumption was made that $\Delta d \approx \Delta s$ for small angles θ, as shown in Fig. 5.

$$\Delta x = \Delta s \cos(\theta + \Delta\theta / 2) \tag{3.5}$$

$$\Delta y = \Delta s \sin(\theta + \Delta\theta / 2) \tag{3.6}$$

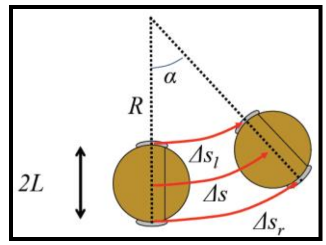

Fig. 3. A wheeled robot of length 2L with each wheel translating some distance **Δs**. [1]

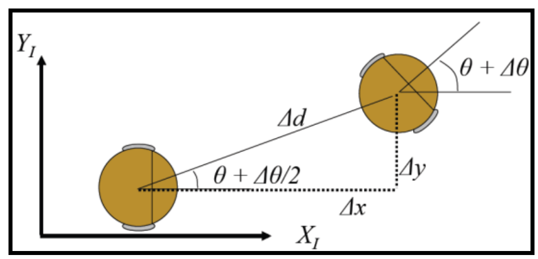

Fig. 4. The Δy and Δx components of displacement can be determined based on the total distance Δd traveled and the heading angle θ. [1]

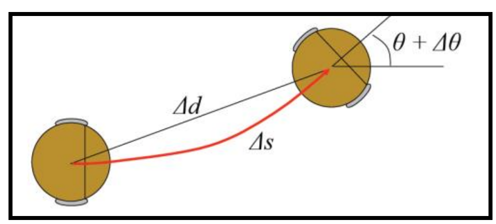

Fig. 5. For small θ, $\Delta d \approx \Delta s$. [1]

IV. Control Design

The kinematic model described above was implemented to predict the position of the Jaguar based on odometry. The sensors and predictions are updated at 20 Hz in the control_loop in Fig. 6.

```
void function control_loop()
  update_encoder_measurements()
  predict_motion()
  update_global_position()
  wait 50ms
end
```

Fig. 6. Psuedocode for the main control loop operated by the Jaguar. The loop currently runs at 20 Hz.

```
void function predict_motion()
  for each wheel:
    Δd = encoder_current - encoder_last
    if rollover is detected:
      correct for rollover in encoder
    implement (3.1) or (3.2) //Δs1/r
  implement (3.3) //Δθ
  implement (3.4) //Δs
end
```

Fig. 7. Pseudocode for predict_motion(), which implements the kinematic model described in Section III.

```
void function update_global_position()
  implement (3.5) //Δx
  implement (3.6) //Δy

  global x += Δx
  global y += Δy
  global θ += Δθ

  if θ ∉ [-π, π]:
    map θ to -π to π
end
```

Fig. 8. Pseudocode for update_global_position, which localizes the Jaguar by integrating odometry measurements made by predict_motion()

After updating the new encoder measurements, the control loop calls functions in Fig. 7 and Fig. 8 to calculate the robot's predicted local motion, then and integrate the motion into its global position. The global variables x, y and θ refer to the global position of the Jaguar.

V. Method

Three sets of experiments were conducted: actual rotation vs. predicted rotation in the lab, actual translation vs. predicted translation in the lab, and actual translation vs. predicted translation outdoors on concrete and grass.

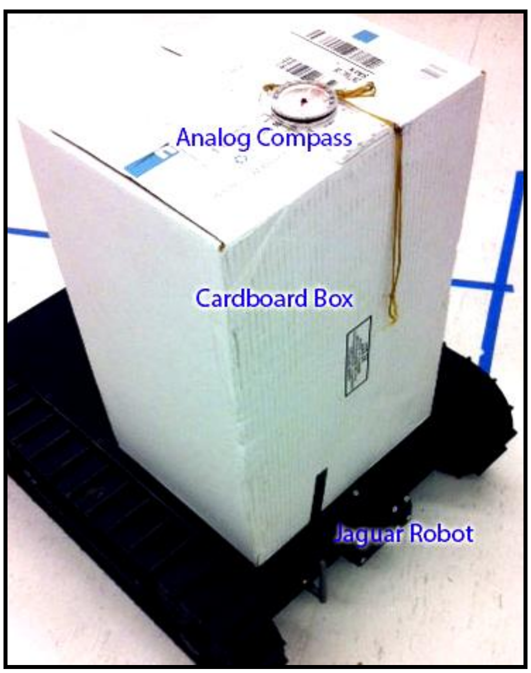

Fig. 9. Jaguar heading measurement compass setup.

A. Continuous Rotation (Indoor)

An analog compass was aligned with the front of the Jaguar and an initial angle measurement was recorded. The compass was taped on a cardboard box approximately 0.5m above the robot in order to isolate the compass from any magnetic interference from the robot's motors. The box was removed, and the Jaguar was instructed to rotate in place a set number of times based on odometry. The analog compass was repositioned as before and a final angle measurement was recorded. The actual rotation of the robot was found by taking the difference between this final angle measurement and the initial angle measurement, and was compared with the Jaguar's calculated angle based on odometry. This test was repeated for rotations ranging from 1π to 20π with increments of 1π. The rotation of 20π was repeated 18 times so that random error distribution could be determined. The setup for this test is shown in Fig. 9.

Fig. 10. Alignment of the Jaguar Robot to the coordinate frame. Center alignment (left) and side alignment (right).

B. x and y Translation (Indoor)

The Jaguar was aligned with a coordinate frame (made of blue tape on the floor). The alignment technique involved squaring a ruler to the front sides and center (illustrated in Fig. 10) to ensure the robot began at the exact same location and orientation each time. The Jaguar is instructed to move forward for 1 or 2.5 meters. Its predicted x and y position based on odometry were recorded. The actual x and y position was measured using a meterstick aligned with the coordinate frame on the floor. The test was repeated for backwards motion.

C. x Translation (Concrete)

Tape was used to mark 1 meter increments on a concrete sidewalk next to a grassy area. The Jaguar was aligned with the sidewalk on the concrete and instructed to move forward for a distance ranging from 0.5 meters to 5 meters with 0.5 meter increments. The actual x distance travelled by the robot was measured using the tape marks and a meterstick. This was compared with the x distance predicted by the Jaguar using odometry.

Fig. 11. Alignment of Jaguar on concrete outdoors.

VI. Results and Discussion

The results of the three experiments are presented in this section: the systematic and random error of indoor rotation, indoor *x* and *y* displacement, and outdoor *x* displacements.

A. Continuous Rotation (indoor)

Fig. 12 shows actual rotation plotted against the rotation predicted by odometry. The slope of the linear fit is 0.875 whereas perfect rotation estimation would produce a fit with slope 1. This suggests that there is systematic error in the odometry measurements that accumulates over time at a rate of 0.125 radians for every 1 radian the Jaguar is instructed to rotate. A possible cause for this systematic error was an inaccurate measurement of the effective radius of the Jaguar, L_{robot}. Error due to uncertainty in measurement from the compass was 0.05 radians, negligible compared to the systematic error and random error.

Fig. 14 shows the random error that occurs for an average rotation of 20.1π over 18 trials. A Gaussian curve is fitted over the histogram to describe the approximate probability distribution of the Jaguar's random error in rotation. The mean is offset from 0 due to the systematic error shown in Fig. 12. From this plot we can see a standard deviation of 2.94 radians. This means that 95% of the error around the mean rotation of 20.1π will be within ±5.88 radians of the mean. The error due to uncertainty in measurement of 0.05 radians is again negligible compared to the effects of random error.

Together, Fig. 12 and Fig. 14 effectively characterize the error of rotation indoors. Systematic error steadily increases with a slope of 0.125, and random error also increases at a rate that we were unable to determine without collecting more data. It is clear, though, that systematic error and random error both become significant at 20.1π rotations. For this rotation, the systematic error has accumulated to 7.89 radians, even more than the random error contribution of 5.88 radians.

B. x and y Translation (indoor)

Experiments were performed to determine the error in the *x* and *y* global translation of the Jaguar robot. This involved measuring the estimated distance traveled and the actual distance traveled, and analyzing the error (estimated – actual). The error in the *x* translation will be discussed first. Following that, the error in the *y* translation at different *x* displacements will be discussed.

1) Systematic error/calibration error of x translation

In a perfectly calibrated motion estimation model, the average actual displacement should tend to equal the estimated displacement with a 1:1 ratio. However, Fig. 15 shows a 0.91:1 ratio of actual:estimated *x* displacement. This systematic error might originate from poorly calibrated wheel diameter values in the kinematic model used. The equation for Δs in (3.4) determines the forward displacement of the robot at each clock cycle, and uses calibrated values of L_{wheel} from (3.1) and (3.2). These values were measured directly from the diameter of the wheels on the tracks. However, since they are tracks, and not wheels as our model assumed, the "effective" wheel radius may be different. Refer to the discussion in section VIII on how to use this ratio to recalibrate the kinematic model.

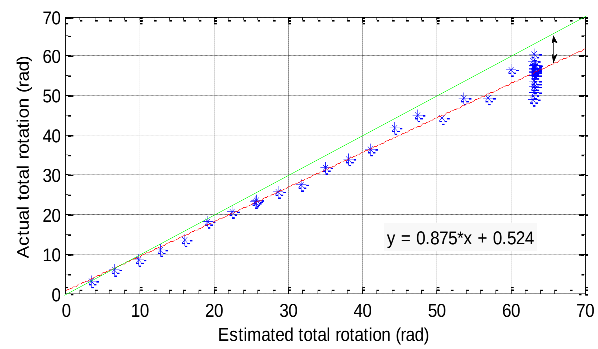

Fig. 12. Estimated vs. actual total rotation of the Jaguar robot, indoors, showing a linear trend (red). The green line, with slope of 1, is what should occur; ideally, the estimated should equal the actual.

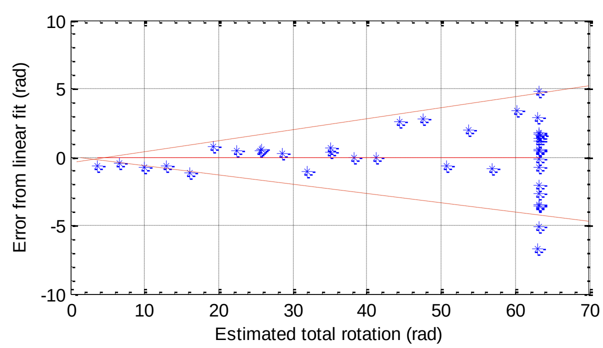

Fig. 13. Residual plot of Fig. 12, showing the increasing random error of Jaguar's continuous rotation.

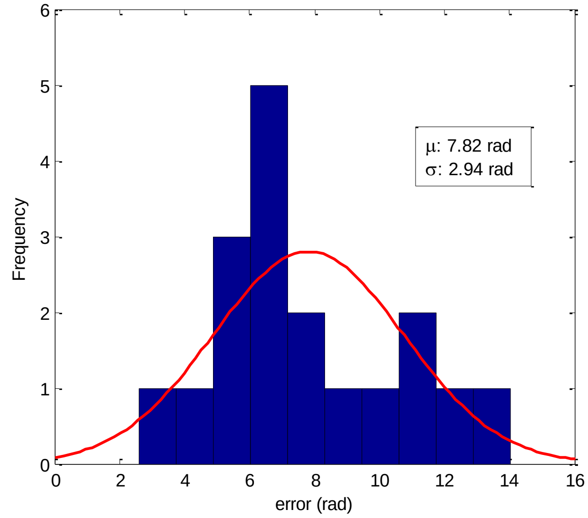

Fig. 14. Histogram plot of the total rotation error at 20π, with a Gaussian distribution fit of the error of standard deviation 2.94 rad and mean 7.82 rad.

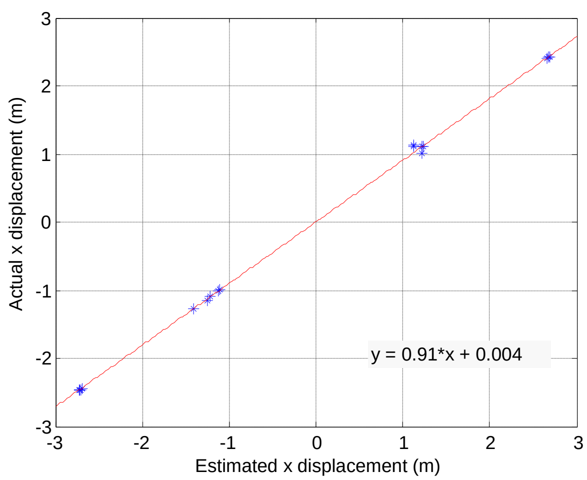

Fig. 15. Estimated *x* displacement vs. actual *x* displacement, showing a systematic error of slope 0.91 where a correctly calibrated system should give a slope of 1.00. The y-intercept, 0.004 m, is negligible given the uncertainty of the measurement with a ruler.

2) Systematic drift error in y translation

As illustrated by the exposure photo in the Introduction (Fig. 2), the drift in the *y* coordinate over time is a main source of error. This drift is far more significant than the drift in the x coordinate. Analytically, this makes sense due to the equations for Δx and Δy in (3.5) and (3.6). Notice how a noisy angle in the sine function in Δy corresponds to a larger error than would a noisy angle in the cosine function in Δx. The random error of Δy can be assumed to have a Gaussian distribution (Siegwart et. al).

The systematic error involved in the drift of the *y* displacement is shown in Fig. 16 by the slope of 0.028. This means for every meter traveled straight forward in the *x* direction, the robot's motion estimation model will have an error of, on average, 2.8cm in the positive Y direction. The robot has a tendency to curve left. This systematic error may come from several causes; it might be caused by the tendency for one side of the robot to slip more, the uneven distribution of mass in the robot, or perhaps a physical misalignment of the tracks or motor on the robot. A straight line path in the motion estimation model may be a circular path in reality.

Similar to Fig. 16, Fig. 17 shows the error in the *y* displacement as the robot goes in reverse. The larger slope, 0.091, suggests that, on average, the robot curves more when going backwards. However, there may not be enough data to substantiate this claim, since the r-squared value is 0.77. This requires further investigation.

3) Random noise and accumalitive drift in y translation

In addition to the systematic error involved in the *y* translation, there is also significant random error shown by the disparity of the points from the linear fit line. These random errors are shown by the residual plots in Fig. 18 and Fig. 19.

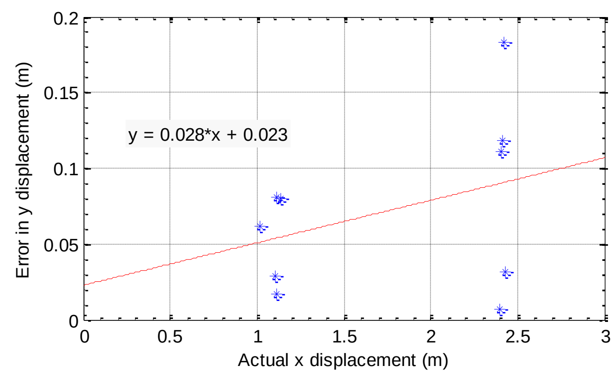

Fig. 16. Forward *x* displacement vs. the error (estimated – actual) in the *y* displacement, showing systematic error with approximate slope of 0.028—there is a tendency for the Jaguar to lean in the positive y direction. The y-intercept of 0.023m suggests that perhaps the systematic error is not linear. However, more data over a larger range would be required to make a qualified judgment.

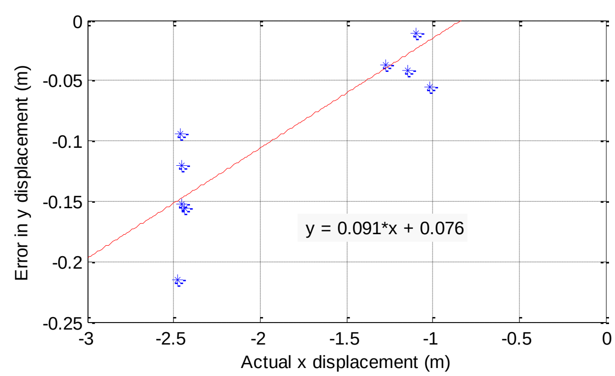

Fig. 17. Error in *y* displacement in the reverse *x* direction, with $R^2 = 0.77$

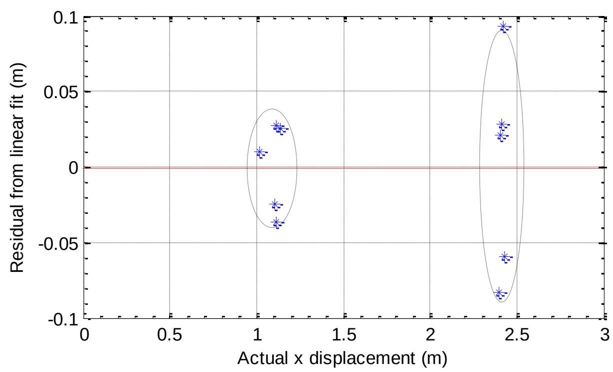

Fig. 18. Residual plot of Fig. 16 showing random error normally distributed around the linear fit. The sample σ at 1.1m is approximately σ = 0.03m, and at 2.5m is σ = 0.07m

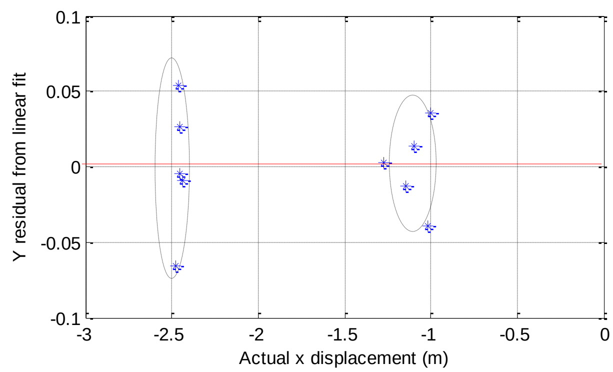

Fig. 19. Residual plot of Fig. 17 showing random error normally distributed around the linear fit. The sample standard deviation at 1.1m is σ = 0.03m and at 2.5m is σ = 0.07m.

The random error of the *y* displacement of the robot for travelling 1.1 meter in the *x* direction, both forwards and in reverse, can be modeled as a random error with normal distribution of sample standard deviation σ = 0.03m. Similarly, at 2.5 meters, the standard deviation is σ = 0.07m. Although only 5 data points were collected on each distance, the calculated standard deviation seems to be consistent, as seen by the ellipses. From the two distances, it seems as though the σ of the random error in *y* displacement increases approximately linearly over *x* displacement: 0.03m each meter. However, there is too little data to effectively justify that claim. Despite that, this standard deviation can be very useful in calculating the accumulated random error over time.

C. *x Translation (Concrete and grass)*

In addition to characterizing the error of Jaguar in the lab indoors, the systematic error of the *x* displacement on concrete and grass is also characterized, shown in Fig. 20. The systematic error on the grass and concrete is significantly similar to the systematic in the indoors, within 15% (or approximately 1cm). The difference is not significant enough to draw any meaningful conclusions on how the surface of concrete, grass, or indoors affects the systematic error in *x* displacement.

Ideally, the random error in *y* displacement on different terrains should be compared. However, due to time limitations, these experiments were not conducted. This requires further investigation.

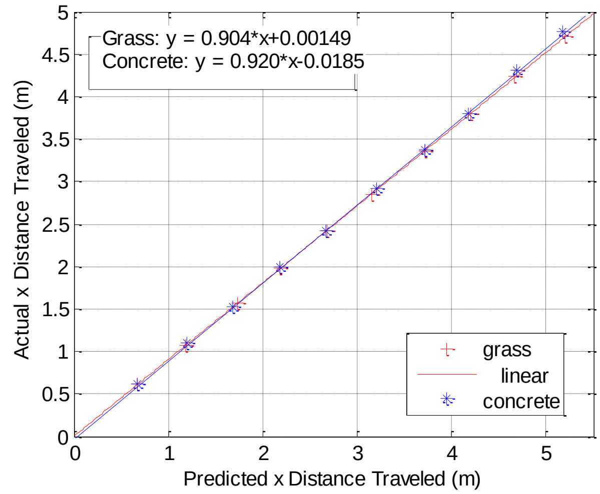

Fig. 20. Plot of predicted x displacement with actual x distance traveled. This plot shows a systematic error with -0.094 for each meter predicted on grass and -0.080 for each meter predicted on concrete.

VII. *Summary of Results*

The summary of the results is shown in the TABLE I. The uncertainty of each value was not analytically calculated as there was not enough data to properly use analytic techniques to significantly determine the uncertainty.

TABLE I. SUMMARY OF KEY ODOMETRY ERROR RESULTS

	Systematic error (actual/predicted)	**Systematic Error (error/predicted)**	**Random error sample standard deviation (σ)**
Rotation (Indoors)	0.875 rad/rad ± 0.005	0.125rad/rad ± 0.005	2.94 rad @ 20π ± 0.05
x translation (Indoors)	0.905 m/m ± 0.005	0.095rad/rad ± 0.005	*negligible*
y translation (Indoors)	*N/A*	0.03 m/m ±0.01 @ forward 0.09 m/m ±0.01 @ reverse	0.03 rad @ 1.1m ± 0.01 0.07 rad @ 2.5m ± 0.01
x translation (Concrete)	0.920m/m ± 0.005	0.080m/m ± 0.005	*negligible*
x translation (Grass)	0.904m/m ± 0.005	0.096m/m ± 0.005	*negligible*

[a] The uncertainties of the systematic error are estimated based on the measurement error of each trial and the closeness of the linear fit lines

VIII. CORRECTION TO MODEL

By using the systematic errors determined in the previous section, we can modify the constants used the kinematic model to eliminate the systematic error.

First, using the systematic error of x displacement to modify L_{wheel} in (3.1) and (3.2), redisplayed below:

$$\Delta s_r = 2\pi L_{wheel} \frac{\Delta d_r}{D_{rev}}.$$

The new radius of the wheel, L_{wheel} , is the old L_{wheel} = 0.28 divided by the systematic error of 0.91:

$$L_{wheel,new} = L_{wheel,old} / 0.91 = 0.309\text{m} \quad (3.7)$$

Similarly, the new L_{robot} in (3.3), redisplayed below, is divided by 0.91, to uncorrect the new L_{wheel}, then multiplied by 0.875,

$$\Delta\theta = \frac{\Delta s_r - \Delta s_l}{2L_{robot}}.$$

So, following, we can determine the new radius of the robot, L_{robot}.

$$L_{robot,new} = L_{robot,old} / 0.91 * 0.875 = 0.232\text{m} \quad (3.8)$$

With the new constants, we can obtain a much better estimated motion. This is illustrated in the figure below. An iPhone taped to the Jaguar, running the app “SensorLog” by Bernd Thomas, provided a time-logged value of the Jaguar’s rotation. This logged data was compared with the logged data from Jaguar.

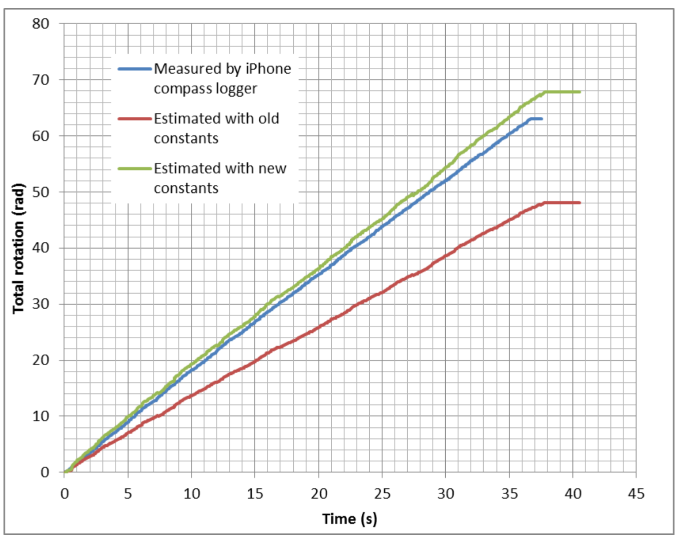

Fig. 21. Comparison of old model with new model constants with continuous stationary rotation. Notice the improved estimation.

IX. CONCLUSION

The results show that odometry alone cannot be relied upon to localize the Jaguar’s position or orientation. The systematic error in rotation and x displacement were characterized to a two significant figure of certainty. The systematic error in y displacement—how much the robot systematically curves—requires further investigation. Additionally, further experimentation in characterizing the random error could prove valuable in obtaining a higher precision of the sigma of the normally distributed random error in y displacement and in rotation.

From the rotation experiment conducted indoors, the random error distribution was determined only around 20.1π rotations. However, random error accumulates as the Jaguar rotates, so collecting more data would allow us to determine the rate at which random error accumulates—whether it’s linear, polynomial, or exponential.

One issue we did not expect when we set up the Jaguar to rotate outdoors was that it could not turn in place on concrete or grass. The static friction of coefficient was too high anywhere other than tiled floors to rotate in place. For future labs and experiments that take place outdoors, the odometry error data we collected for rotation will not be very useful. We would find it more useful to conduct further odometry tests outdoors by rotating just one track, as this is the motion the Jaguar Lite will use to rotate outdoors.

By the kinematic model, we would assume that the errors in rotation and in translation are a simple vector addition. However, that may not be true. There may be more random slippage when the robot is rotating stationary than when it is travelling in a wide curve. To characterize this error, more data is required, and a method to map the robot’s actual path would need to be devised.

Currently, the calibration correction to the kinematic model does not implement the systematic error from the y displacement, which showed that the robot’s motion tends to curve. Implementing this calibration may be useful to ensure the robot would go straight. However, since the random error of the y displacement may be on the same order of magnitude as the systematic error, this additional calibration may not prove to be as useful.

Another improvement could be to consider how different velocities or acceleration of the robot may contribute to different error characteristics. Maybe if the robot goes slower, there would be less slippage, causing a tighter distribution of random error. Furthermore, the robot is currently instructed to stop immediately. If the deceleration is gradual—if it comes to a stop gradually—there may be less slippage and hence the x error may be less. Additionally, since a lower battery life decreases the maximum torque of the motor, a lower battery life also decreases maximum acceleration. Hence, battery life may also affect the difference in the error characteristics.

Overall, the results collected in this lab allowed effective recalibration to the Jaguar’s kinematic model. They also allowed us to better understand the random errors involved in rotation and translation of the Jaguar robot. The lab also demonstrated that further investigation is required to establish a more concrete characterization of the random normal distribution of each global coordinate. Using odometry alone cannot reliably localize the Jaguar robot due to too many random sources of error. If the ultimate goal is to enable autonomous control of the Jaguar, a more reliable method of localization, perhaps involving the laser range finder, should be considered.

X. ACKNOWLEDGEMENTS

Special thanks to Taylor Peterson and Hannah Kastein for sharing their data of the indoors *x* and *y* displacement measurements, and to Laruen Lieu and Joshua Vasquez for sharing their data of the outdoors *x* displacement. Also, special thanks to Dr. Chris Clark for providing the diagrams in Fig. 3, Fig. 4 and Fig. 5 on his power point class lectures.

XI. REFERENCES

[1] R. Siegwart, I. Nourbakhsh, D. Scaramuzza, Introduction to Autonomous Mobile Robots, 2nd ed., The MIT Press : Cambridge, 2011.